Fuel 352 (2023) 129013

Contents lists available at ScienceDirect

Fuel

journal homepage: www.elsevier.com/locate/fuel

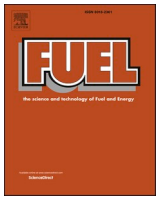

Full Length Article

Investigations of the extended Eddy Dissipation Concept formulation for weakly turbulent and slow chemistry flames

Bima A. Putra *, Ivar S. Ertesvåg

Department of Energy and Process Engineering, NTNU Norwegian of Science and Technology, Kolbjørn Hejes vei 1b, NO 7491 Trondheim, Norway

ARTICLE INFO

Keywords:
Turbulence
Combustion
Modeling
CFD
RANS
OpenFOAM
EDC
MILD flame

ABSTRACT

Recent extensions of the Eddy Dissipation Concept (EDC) are investigated with the purpose of analysing the importance of model limiters to the EDC performance when predicting Moderate and Intense Low-oxygen Dilution (MILD) flames. These limiters are associated with the mass fraction of fine structure regions, turbulence Damköhler number (*Da*), and turbulence Reynolds number (*Re*). The method is Reynolds Averaged Navier Stokes computation using OpenFOAM v.7 combined with the modified steady-state solver edcSimpleSMOKE. The results show that increasing the upper limit of fine structure region close to unity influences flame temperature, which could critically affect the turbulence *Da* and *Re* fields. The minimum constraint of turbulence *Da* plays a significant role in distributing reaction, thus imitating the behaviour of MILD flames. Tuning this constraint is also crucial for the accuracy of the model extension since it can allow nullifying or maximising modification effects for weakly turbulent and slow chemistry flames. The limit of turbulence *Re* is analysed in relation to turbulence modelling. Evaluation against a conventional turbulent flame demonstrates that the extended EDC underpredicts turbulence *Da* field, allowing similar modification to that applied in MILD condition.

1. Introduction

The Eddy Dissipation Concept (EDC) for turbulent combustion is a mathematical model used to predict turbulence-chemistry interactions [1]. This model was originally developed as a Computational Fluid Dynamics (CFD) tool for turbulent combustion in the framework of Reynolds Averaged Navier Stokes (RANS) computation [2]. Its wide range of applicability for both premixed and non-premixed flame has made this model attractive in academic and industrial work. Different levels of complexity can be applied to the EDC regarding the reaction mechanism. Despite its wide functionality, attention has been drawn to the development of EDC with the purpose of modelling Moderate or Intense Low oxygen Diluted (MILD) combustion in different lab-scale experimental configurations, such as jet-in-hot-coflow [3,4] and gas furnaces with preheated air [5] or without preheated air [6,7].

MILD flames have become important for engineers and scientists moving towards a more efficient and environmentally friendly combustion technology. The main characteristic of such flames is to have a relatively low and uniform flame temperature, thus reducing pollutants such as CO, NO_x, and soot [8,9]. MILD combustion also becomes attractive for application using carbon–neutral and low-calorific fuel application [8], as well as hydrogen blends with natural gas [10]. These flames are also characterized by the preheated reactant with low oxygen concentration [11], allowing the chemical time scales to be comparable with the fluid time scales (e.g., turbulent mixing time scale). The mechanism for preheating reactant could be using a secondary burner [12,13], a recuperator [14], recirculating flue gas [15], or an electric furnace [16,17]. These experimental setups were constructed to investigate non-premixed flame, but a cylindrical furnace equipped with a premixing chamber was employed to generate premixed propane-air MILD combustion [18].

According to [19], EDC is the preferable option for simulating MILD combustion. EDC can be applied with a Perfectly Stirred Reactor (PSR) model to estimate the chemistry rate, and this approach was found to be appropriate for modelling reaction zones under MILD conditions [20]. Successful implementation of EDC in such conditions was, however, followed by some modifications to remedy the overprediction of the overall reaction rate by the standard EDC. Initially, relatively simple modifications were proposed, which was to change the model constants. Numerous works have employed this method, and they have been summarized and critically reviewed by Ertesvåg [21]. Among others, a high level of accuracy was obtained by applying inverse problem

* Corresponding author.
E-mail addresses: bima.a.putra@ntnu.no (B.A. Putra), ivar.s.ertesvag@ntnu.no (I.S. Ertesvåg).

https://doi.org/10.1016/j.fuel.2023.129013
Received 30 March 2023; Received in revised form 2 June 2023; Accepted 14 June 2023

methodology to determine new model constants [22] or with a method linking constants to the reaction rate [6]. Nevertheless, the generality of new values of constants can be an issue as it was found, for instance, that conventional flames were predicted similar to MILD flames when using the new constants [23]. To solve this issue, researchers offered more advanced modifications with the principle of treating the EDC model constants as local variables.

Parente et al. [24] proposed functional expressions such that the model constants were dependent on local turbulence Reynolds number Re_τ and Damköhler number Da_τ. The functional expressions were based on an idea of using premixed flame quantities such as the laminar flame speed for estimating the reacting structures with large degree of premixing. This approach was supported by the result of a DNS study [25] which demonstrated that MILD reacting structures were highly convoluted and widely distributed. In a revised version by Evans et al. [26], the chemical time scale (for calculating Da_τ) was estimated from the reaction rates of CH_4, H_2, O_2, CO, and CO_2. Romero-Anton et al. [5] proposed an alternative to Parente's formulation by assuming that the fine structure length scale is the same as Kolmogorov length scale, and this version was improved afterwards to consider the interaction between reaction zones [27]. Mardani and Nazari [28] also made a similar attempt with, however, a different expression for the effects of Re_τ and Da_τ, which was in the opposite direction of Parente's formula. Beside modifying the model constant, taking into account molecular diffusion in the species transport equation was found important to improve the accuracy of modelling MILD flames with hydrogen containing fuel [29], and either was molecular diffusion in the energy transport equation [30]. Farokhi and Birouk [31] employed a fractal modelling approach to modify the expression for turbulence intermittency. Afterwards, they proposed a hybrid model [32] by introducing a fractal-based flame surface density approach, and better predictions were achieved in the mixing field.

Experimental data from jet-in-hot coflow flames, such as the Adelaide flames [12] and Delft flames [13], have been used for the validation of the extended EDC. Moreover, experiments in lab-scale gas furnaces [7,14,15] and a micro gas turbine burner [17] were used as references. Experimental data from a pulverized coal furnace operating in MILD regime [33] was used to validate a numerical model using EDC [34].

Numerical studies have been carried out to understand the effect of input parameters on MILD flames. For instance, it was demonstrated that an increase in fuel (methane) temperature reduced NO_x emissions, indicating a better mixing between fuel and oxidizer [16]. Numerical modelling of counterflow MILD flames showed that increasing the oxidizer temperature above 1200K would contribute to an escalated concentration of thermal NO [35]. Another study concluded that the NO_x emission of methane combustion increased as the global air-to-fuel ratio decreased from 2.55 to 1.67 [17]. The addition of diluted CO_2 in the reactants resulted in the reduction of the peak in Da_τ [36]. It was found that a syngas mixture with a high fraction of CO_2 and N_2 exhibited MILD combustion with a low NO_x concentration [7]. Effects of adding methane as a diluent in a syngas mixture varied depending on the H_2/CO ratio [37].

The progress of modelling the MILD flames has inspired the development of fire modelling. A methanol pool fire was numerically studied using an EDC version adopted from the MILD study [38]. Furthermore, underventilated compartment fires share some of the characteristics of MILD flames due to the presence of hot reactants with limited oxygen. Efforts have been made to capture the slow chemistry effects when modelling underventilated fires using infinitely fast chemistry EDC [39,40].

Lewandowski et al. [3,4] proposed an EDC extension that was reported to have a better generality for a wide variety of weakly turbulent MILD flames, compared to the previous modification by Parente et al. [24]. This extension included three features: the first was to treat the EDC model constants as variables that were dependent on Re_τ and Da_τ. The second was to apply the standard EDC when Re_τ fell below a threshold of which the number of levels in the turbulence energy cascade had reduced to one. The third was to revert the EDC formulation to its standard version whenever Da_τ dropped too low. The standard version here refers to the 1996 version of EDC [41] in which the variable reacting fraction (denoted as "Detailed 1" there) is taken into account when calculating the overall reaction rate. The proposed extension model has been validated against the Adelaide flames and the Delft flames. However, there was still a lack of analysis regarding the significance of the third extension feature (the ignition model). Information was also still missing regarding the sensitivity of the combustion model to key limiters, such as the maximum fine structure mass fraction ($\gamma_{\lambda,\max}$) and the minimum Da_τ.

The present work aims to critically study the application of the proposed extension of EDC. This will be an advancement of the previous analyses [21,42]. Apparently, there are improvement potentials in modelling slow chemistry and weakly turbulent flames using EDC. To achieve such improvement, the performance of the current formulation needs to be clarified, and important model settings and assumptions need to be discussed in more detail. A future aim is to modify the existing model to handle reacting flows with weak turbulence and slow chemistry. Two objectives are specified for the present study: The first is to analyse and discuss the impact of introducing the ignition model (Da_τ minimum constraint), and the second is to perform sensitivity analyses on the key limiters. The latter includes an investigation of the impact of having different Re_τ predictions due to using different turbulence models. In addition, discussions will be given to highlight key points to proceed with the development of the EDC formulation. In Section 2, the relevant theoretical foundation of EDC will be reviewed. Next, Section 3 will describe the developed CFD model setup as well as the experimental test cases found in literature for investigation. Section 4 will present the work for the first objective, while Section 5-7 are assigned for the second objective. Overall discussions and conclusions will be given in Section 8 and 9, respectively.

2. The Eddy disspiation Concept (EDC)

2.1. Fundamental theory of fine structure

The Eddy Dissipation Concept (EDC) principally assumes that for highly turbulent flow, the chemical reactions take place in fine structures, i.e., small scales. The size of fine structures is modelled to be in the same order of magnitude as the Kolmogorov length scale. The ratio between the mass fraction of the fine structures and the total mass, γ^*, can be expressed from the turbulence Reynolds number Re_τ and a model constant C_γ, i.e.,

$$\gamma^* = C_\gamma{}^n (Re_\tau)^{-n/4} = C_\gamma{}^n \left(\frac{\nu\varepsilon}{k^2}\right)^{n/4}, \tag{1}$$

where $Re_\tau = k^2/\nu\varepsilon$, ν is the kinematic viscosity, k is turbulence energy and ε is turbulence energy dissipation rate. In this expression, $n = 2$ or 3 has been applied throughout the development of EDC [41,43]. EDC also specifies the mass fraction of the fine structure region, i.e., $\gamma_\lambda = (\gamma^*)^{1/n}$.

Another important EDC parameter is the mass exchange rate of the fine structures divided by their mass, which is modelled as

$$\dot{m}^* = \frac{1}{C_\tau}\left(\frac{\varepsilon}{\nu}\right)^{1/2}. \tag{2}$$

The secondary constants C_γ and C_τ are derived from the primary constants C_{D1} and C_{D2} [21,44]. The secondary constants have been used as the tuning parameters for adjusting the overprediction of the reaction rate in MILD flame simulations [6,45]. Ertesvåg [21] summarized the suggested changes in the model constants and analysed that some changes have led to deviations from the EDC cascade theory, such as a considerably larger or smaller fine structure than the Kolmogorov length

scale.

In the EDC theory, the distributed fine structures are treated as an ideal reactor, i.e., transient Perfectly Stirred Reactor (PSR). Assuming a steady-state solution for the reactor, the reaction rate of species k can be iteratively calculated from the mass balance,

$$R_k^* = \rho^* \frac{\left(Y_k^* - Y_k^o\right)}{\tau^*}, \tag{3}$$

where ρ is the fluid density, Y_k is the mass fraction of species k, and the superscripts * and o denote the reactor and the surroundings, respectively. The residence time of the reactor is the reciprocal of $\dot{m}^*$, i.e., $\tau^* = 1/\dot{m}^*$. Eq. (3) here can be followed by an assumption that the reactor is adiabatic and isobaric. The use of a PSR model for simulating combustion has enabled a mechanism for aerodynamical extinction at a high strain rate [46]. However, at a low strain rate, the prediction of the aerodynamic extinction can be an issue since the turbulence model can overpredict the mixing time scale.

The relation between the mean quantities (denoted by the overbar) and the reactor quantities is expressed as

$$\overline{R}_k = \bar{\rho}\chi\gamma^* \frac{\left(Y_k^* - Y_k^o\right)}{\tau^*}, \tag{4}$$

where Y_k^* is usually substituted from the steady-state solution of Eq. (3). Eq. (4) introduces χ, the reacting fraction. The expression of χ follows the version of Gran and Magnussen [41], which was essentially proposed by Magnussen [1]. This expression was reformulated by Ertesvåg [21] as

$$\chi = \min\left\{\frac{1}{\lambda}, \lambda\right\} \cdot \min\left\{\frac{c}{\gamma_\lambda}, 1\right\} \cdot \min\left\{\frac{\gamma_\lambda}{1-c}, 1\right\}, \tag{5}$$

where λ is the excess air ratio (reciprocal of equivalence ratio), and c is the extent of reaction, estimated from the mean mass fractions of reactants and products of a one-step global fuel-oxidizer reaction. This χ expression is of interest as it was found significant in low Reynolds number flames [42]. The surroundings quantity Y_k^o is computed from the mean and reactor quantity, i.e., $Y_k^o = \left(\widetilde{Y}_k - \chi\gamma^* Y_k^*\right) \Big/ \left(1 - \chi\gamma^*\right)$ [21], and Eq. (4) can be rewritten as

$$\overline{R}_k = F\bar{\rho}\left(\frac{\varepsilon}{\nu}\right)^{1/2}\left(Y_k^* - \widetilde{Y}_k\right), \tag{6}$$

where $F = \chi\gamma^*/(C_\tau(1-\chi\gamma^*))$ is termed as "the EDC factor", which is dimensionless. F will increase with γ^* and finally reaches its maximum value of 2.5 when $\gamma^* = 1$ or $Re_\tau = 21$. Practically, EDC solvers may enable users to set a maximum limit ($\gamma_{\lambda,\max}$), which is an arbitrary number smaller than one, with the purpose of avoiding zero or a negative denominator in F.

The definition of "standard EDC" follows the work of Ertesvåg [47], which is to employ Eqs. (4) and (5) with Eq. (1) for γ^* with $n = 2$, $C_\gamma = 2.13$, and Eq. (2) for $\dot{m}^*$ with $C_\tau = 0.4082$, that is, $C_{D1} = 0.135$ and $C_{D2} = 0.5$.

2.2. The extended EDC (v2020)

The extended EDC refers here to the version proposed by Lewandowski et al. [3], hereafter called "v2020 EDC". This version was partly motivated by the work of Parente et al. [24], where the use of locally modified EDC constants was attempted successfully for predicting the Adelaide Flames. The model constants C_γ and C_τ are replaced by new variables, here denoted as $C_{\gamma,p}$ and $C_{\tau,p}$, respectively. These two new variables are functions of Re_τ and Da_τ. More importantly, Da_τ is evaluated from the ratio of the mixing time scale to the chemical time scale, i.e., $Da_\tau = \tau_{\text{mix}}/\tau_c$. The mixing time scale, τ_{mix}, needs to be estimated. One alternative is to use the Kolmogorov time scale [24], i.e.,

$$\tau_\eta = \sqrt{\nu/\varepsilon}. \tag{7}$$

Parente et al. [24] originally proposed the one-step global reaction of methane/air mixture to estimate τ_c. Due to its robustness, Lewandowski et al. [4] adopted the same method in which τ_c is defined as

$$\tau_c = \left\{\left(8.3\cdot 10^5\right)^{-1}\text{s}\right\} \exp\left(15100\text{K}\Big/\widetilde{T}\right), \tag{8}$$

where $\widetilde{T}$ is the mean temperature. Evans et al. [26] argued that this method is fuel-specific and not suitable for finite-rate reactions. Therefore, they proposed to estimate the chemical time scale from formation rates, i.e.

$$\tau_{c,k} = \frac{Y_k^*}{\left|dY_k^*/dt\right|} = \frac{\rho^* Y_k^*}{\left|R_k^*\right|}, \tag{9}$$

where the maximum value of $\tau_{c,k}$ between five major species CH_4, H_2, O_2, CO, and CO_2 was used. Eq. (8) and (9) denote "Variant 1" and "Variant 2", respectively. However, Variant 2 in the present study considers all species in the selected reaction mechanism.

In v2020 EDC, it was proposed to revert $C_{\gamma,p}$ and $C_{\tau,p}$ to their standard values when the turbulence energy cascade falls to one level, i.e., when $Re_\tau = Re_{\tau,\text{limit}} = C_{D2}/{C_{D1}}^2 = 27.8$ [3]. This value was obtained from the secondary EDC constants [3], while the primary constants give 27.4 [47]. The validity of $C_{\gamma,p}$ and $C_{\tau,p}$ at very low Re_τ can be questioned as viscous effect decreases with increasing Re_τ [47]. Furthermore, the modified model was found inadequate for the Delft flames, which have $Re_\tau < 27.8$ in the reaction zone. A minimum constraint was also imposed to Da_τ such that $C_{\gamma,p}$ and $C_{\tau,p}$ again revert to their standard values when $Da_\tau < Da_{\tau,\min}$. The purpose of doing so was to ensure ignition. It was suggested that $Da_{\tau,\min}$ should be varied depending on Re_τ because small improvements can be achived by decreasing $Da_{\tau,\min}$ as much as possible [3]. The variable $Da_{\tau,\min}$ used for computations in [3] is expressed as (M. Lewandowski, personal communication, Jan.-Feb. 2021)

$$Da_{\tau,\min} = 0.01129 + 0.9907^{(Re_\tau + 306)}. \tag{10}$$

The model equation indicates that $Da_{\tau,min}$ increases as the Re_τ decreases. In other words, the combustible mixture becomes more reactive as the turbulence intensity gets low. This concept is in line with the concept of extinction/reignition for premixed pocket eddies [39].

The expression of $\overline{R}_k$ in the v2020 EDC is

$$\overline{R}_k = \begin{cases} \bar{\rho}\gamma_p^* \dot{m}_p^* \left(Y_k^* - Y_k^o\right) & \text{for } Re_\tau > 27.8 \text{ and } Da_\tau > Da_{\tau,\min}, \\ \bar{\rho}\gamma^* \dot{m}^* \chi \left(Y_k^* - Y_k^o\right) & \text{else,} \end{cases} \tag{11}$$

with the formulation

$$\gamma^* = \min\left\{{C_\gamma}^2 (Re_\tau)^{-1/2}, {\gamma_{\lambda,\max}}^2\right\}. \tag{12}$$

The limiting value $\gamma_{\lambda,\max} = 0.7$ is used [45]. Eq. (2) with $C_\tau = C_{\tau,p}$ is used for $\dot{m}_p^*$, and Eq. (12) with $C_\gamma = C_{\gamma,p}$ is used for γ_p^*. The variable χ is employed [41], see Eq. (5).

3. Numerical setup and experimental data

The equimolar CH_4/H_2 jet-in-hot-coflow flames [12], aka. Adelaide flames, were used to investigate the MILD flame modelling. These flames were generated from a burner with a fuel nozzle surrounded by exhaust gas coming from an internal/secondary burner. The Adelaide flames have previously been investigated numerically [4,24,29]. The present study focuses on two cases that have coflows with 3 and 9% O_2 mass fractions, namely HM1 and HM3, respectively. Both flames had a bulk mean jet Reynolds number of 10000. The simulations applied the standard $k-\varepsilon$ model with the Pope correction on ε [48] for a round jet.

However, the effect of using different model variants was also studied such as realizable $k-\varepsilon$ [49], $k-\omega$ SST [50,51] and standard $k-\varepsilon$ [52]. The computational domain and mesh configuration were studied previously [3] and found mesh independent. The radiation heat exchange was neglected as it was minor for the selected flames [4,24,29]. The Kee chemical mechanism (17 species and 58 reactions) [53] was used.

Another reference for MILD flames is the Dutch natural gas jet-in-hot-coflow flames or Delft flames [13]. The burner for these flames was also equipped with a secondary burner to generate hot coflow. The Delft flames have been investigated numerically [42,45]. Different flame configurations have been examined, but this study focuses on a flame with a jet Reynolds number of 4100 (DJHC-I 4100). The fuel was Dutch natural gas composed of 15% N_2, 81% CH_4, and 4% C_2H_6 (by volume). The coflow contained less than 8% oxygen. The standard k-ε model [52] was applied for a round jet. The computational domain and mesh configuration has been previously studied [42] and was found mesh independent. The radiation heat transfer was neglected [42,45]. DRM19 (19 species and 58 reactions) [54] was used for the chemical reaction mechanism. All other simulation parameters are reported in [4].

Besides MILD flames, turbulent jet diffusion flames with a fuel mixture of 33.2% CH_4 / 22.1% H_2 / 44.7% N_2, called DLR flames [55] were also investigated. These flames were set up by a burner with a fuel jet surrounded by coflowing dry air. The DLR flames can be considered as conventional highly turbulent diffusion flames, and investigation using these flames was meant to verify whether the extended EDC would give a prediction similar to that of the standard EDC. This study focuses on a flame configuration in which the exit velocity of the jet was 42.15 m/s (jet Reynolds number of 15200), namely DLR-A. A numerical study of this flame [56] reasoned that the Damköhler number was high, such that the flame falls under the flamelet regime. A two-dimensional axisymmetric domain was created, consisting of 24604 computational elements. The standard k-ε turbulence model with the Pope correction on ε [48] and the P1 radiation model were applied. DRM19 was used for the chemical reaction mechanism.

All simulations were performed using OpenFOAM v.7 combined with the modified steady-state solver edcSimpleSMOKE [57]. Accordingly, all results reported here are steady-state solutions. The OpenSMOKE library [58] was used to solve the chemistry. For MILD flames, multicomponent molecular diffusion was taken into account to improve the accuracy [29]. Setting $\gamma_{\lambda,\max}$ close to unity may lead to a numerical error due to a local temperature beyond the range stored in the library of the thermodynamic properties (250 K $\leq T \leq$ 3000 K). It was found that $\gamma_{\lambda,\max}$ up to 0.95 was still applicable for the MILD flames. However, $\gamma_{\lambda,\max} = 0.7$ was found the maximum for DLR-A.

4. The ignition model

4.1. Background

According to Lewandowski et al. [3], the ignition model, i.e., introducing a minimum value for Da_τ, has played a critical role in ensuring ignition and improving the accuracy of the model. A variable $Da_{\tau,\min}$ was proposed to give an optimum prediction of the Adelaide flames. However, the generality of this expression was not discussed in details. Moreover, it was reported that the locally modified constants had led to full extinction when predicting DJHC-I 4100 despite using the same ignition model.

The purpose of this section is to gain an understanding of the impact of the ignition model. The study will analyse how the ignition model has enabled the distributed reaction zone. For this analysis, the simulation results of HM1 and HM3 using the v2020 EDC will be post-processed. In addition, the ignition model will be tested against DLR-A to elucidate its generality. The issue of total extinction in DJHC-I 4100 will be addressed in Section 6.3, where a parametric study of $Da_{\tau,\min}$ will be carried out.

4.2. The Adelaide flame, HM1

The v2020 EDC with $\gamma_{\lambda,\max} = 0.95$ was used to study the ignition model. Two different reaction zones were evident in the temperature contour from the simulated HM1 flame, as depicted in Fig. 1a. The high-temperature flame upstream was a result of the standard EDC at $Re_\tau <$ 27.8 (Zone 1). Meanwhile, the low-temperature flame downstream (Zone 2) was where the locally modified constants play a role together with the ignition model. This observation was supported by the Re_τ profile along the monitoring line across the zone boundary, depicted in Fig. 1b. It is seen that Re_τ increases downstream, resulting in a transition towards using the standard EDC. The boundary between the two zones can be made apparent in the Re_τ field. The prediction of the mean reaction rate in Zone 1 and 2 was considerably different, resulting in a rapid drop in temperature. An immediate switch (without any smoothing transition functions) of the $\overline{R}_k$ formula at $Re_\tau = 27.8$ could be a factor behind the significant temperature gradient. It is worth mentioning that the local mesh resolution in Zone 2 was lower than in Zone 1 because the mesh density decreases along the axial and radial distance. For example, around the monitoring line, the cells expand uniformly with expansion ratios of 1.006 in z direction and 1.023 in r direction.

It could be argued that the simulation result near the transition zone was sensitive to the prediction of Re_τ. The selection of the turbulence model was primarily responsible for the Re_τ prediction. However, other parameters like $\gamma_{\lambda,\max}$ may also play a critical role. In Section 5.2, the sensitivity of critical model setups on the Re_τ prediction will be investigated.

It was reported in the previous study of HM1 [4] that the radial profile of the OH mass fraction had only one peak, indicating the location of the primary reaction zone. In the present study, two peaks were, however, visible in the profile of volumetric reaction heat release ($\dot{Q}/V$), as seen in Fig. 2a. The $\dot{Q}/V$ profile is plotted at $z = 250$ mm for better visibility as the distance between the two peaks became larger when moving downstream. The second peak was located closer to the jet centre. Hereafter, the location of the second peak will be called the "secondary reaction zone". Interestingly, the peak of the mass fraction of CO took place in the secondary reaction zone. The fuel-rich combustion might be responsible for generating the maximum CO. Moreover, it was confirmed that the ignition model triggered the secondary reaction. The value of Da_τ was found smaller than $Da_{\tau,\min}$ near the secondary reaction zone. It can be argued that the hot combustible mixture here only requires the reignition criterion $Da_\tau < Da_{\tau,\min}$. The flame exhibited premixed flame characteristics. A similar argument was also given for another Da_τ-based reignition model by Ren et al. [40], in which the reaction time scale was no longer controlled by the mixing rate but by the laminar burning velocity.

The secondary reaction zone may not be well validated regarding its presence and location. Although turbulence-chemistry interactions in MILD flames may cause unsteady phenomena such as local extinction and ignition [59], the present simulations here only represent statistical results (Favre averaged). Nevertheless, the finding of a secondary reaction zone can be important for the model itself, because it explains the uniform temperature distribution.

4.3. The DLR-A flame

The use of χ in Eq. (5) resulted in a lifted flame. This result was attributed to the fact that to enable reactions, χ requires the coexistence of global reactant and products. This requirement could not be fulfilled near the jet exit. The local mesh resolution in the near field of the nozzle was approximately 2 cells/mm in r direction. This mesh might largely influence the result because $\min\{\lambda^{-1}, \lambda\}$ in Eq. (5) was found sensitive to the mesh resolution [42]. The lifting flame issue deserves further investigation but is considered out of scope in the present work. To avoid this issue, $\chi = 1$ will be used in the following when applying the

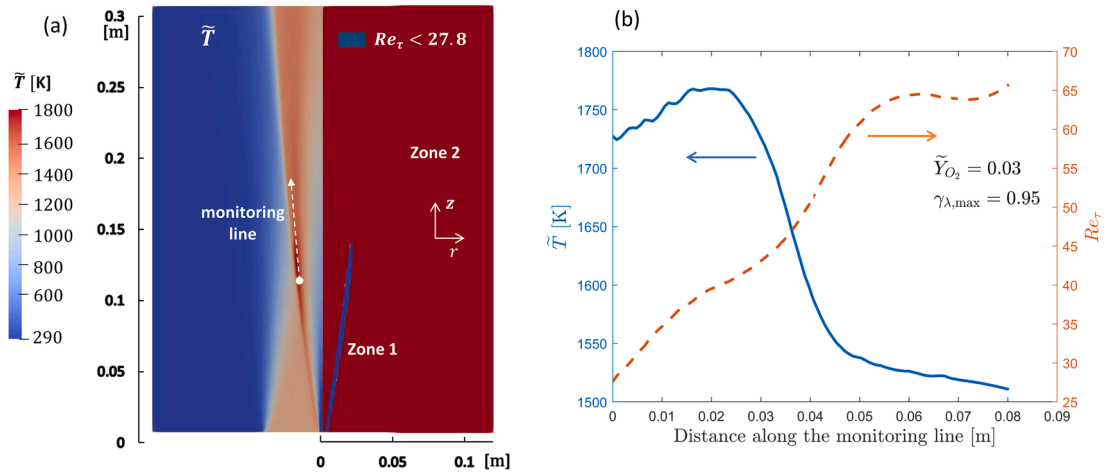

Fig. 1. (a) Temperature andRe_τ field of simulated HM1 using v2020 EDC with $\gamma_{\lambda,\max} = 0.95$. (b) Temperature and Re_τ profile along a monitoring line from (100,16) to (180,22) mm. The location of the monitoring line is shown in (a).

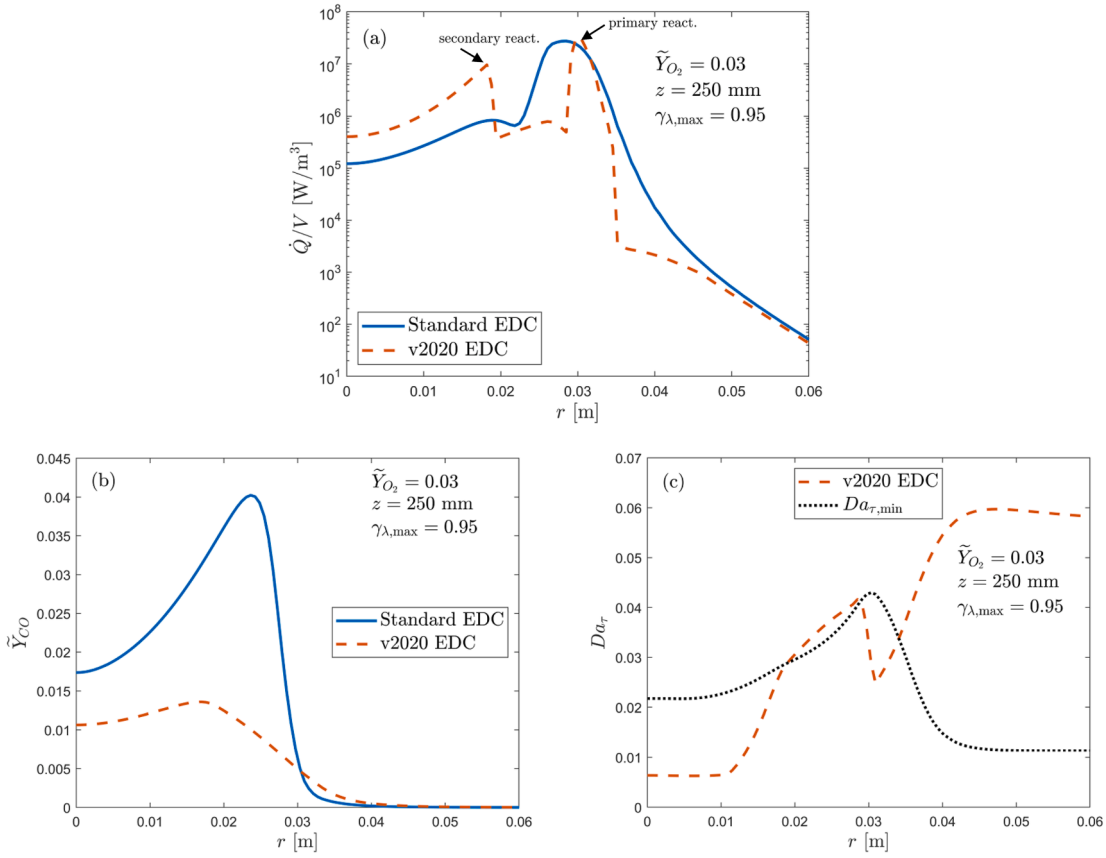

Fig. 2. Radial profiles of (a) volumetric reaction heat release, (b) CO mass fraction, and (c) turbulence Damköhler number, all at $z = 250$ mm. Comparison of standard and v2020 EDC, HM1 flame. $\gamma_{\lambda,\max} = 0.95$ for all cases.

standard and v2020 EDC for DLR-A.

The solution by the v2020 EDC with $\chi = 1$ showed that the ignition model had prevented the flame from complete extinction. The reduction of OH mean reaction rate at $z/d = 20$ after applying v2020 EDC with and without the ignition model is shown in Fig. 3a. The overall flame temperature obtained from v2020 EDC was lower than that of the standard EDC, as demonstrated in Fig. 3b.

The solution of the standard EDC was post-processed to check whether the flame is identified as slow and weakly turbulent. Re_τ and Da_τ are plotted radially at $z/d = 20$ from the nozzle exit, as depicted in Fig. 4a. It is visible that Re_τ could drop to less than 200 when approaching the reaction zone ($2.5 < r/d < 3.5$). The Re_τ field in Fig. 4b qualitatively suggests that the reaction zone near the nozzle exit has relatively low turbulence. Here, the reaction zone can be very close to the outer layer of the jet, which has a low turbulence viscosity. Furthermore, the Da_τ field generally showed a low value (<1) across the reaction zone.

To check to what extent the v2020 EDC could affect the simulation, the EDC factor F is plotted in Fig. 5. Two different F profiles are presented due the two variants of τ_c. An important observation was that

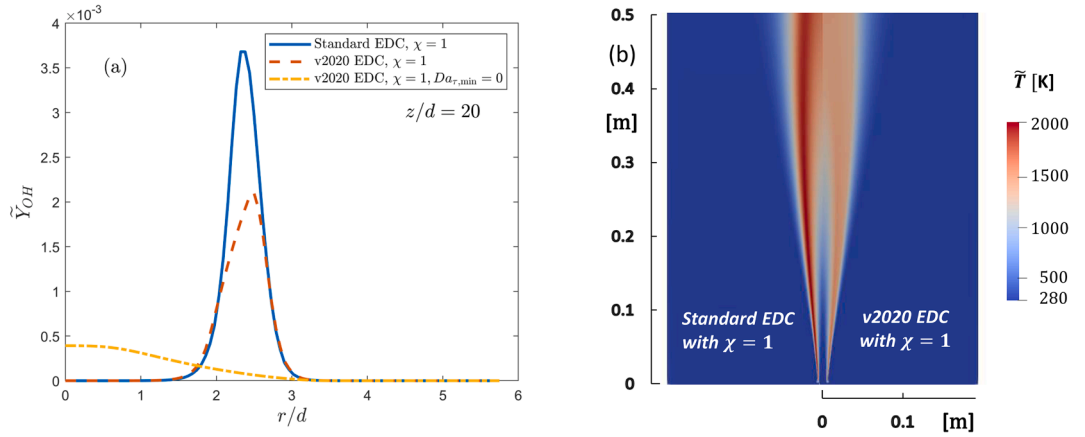

Fig. 3. (a) Radial profiles of OH mass fraction of simulated DLR-A at $z/d = 20$. (b) Temperature field obtained from standard EDC and v2020 EDC. $\chi = 1$ for all cases.

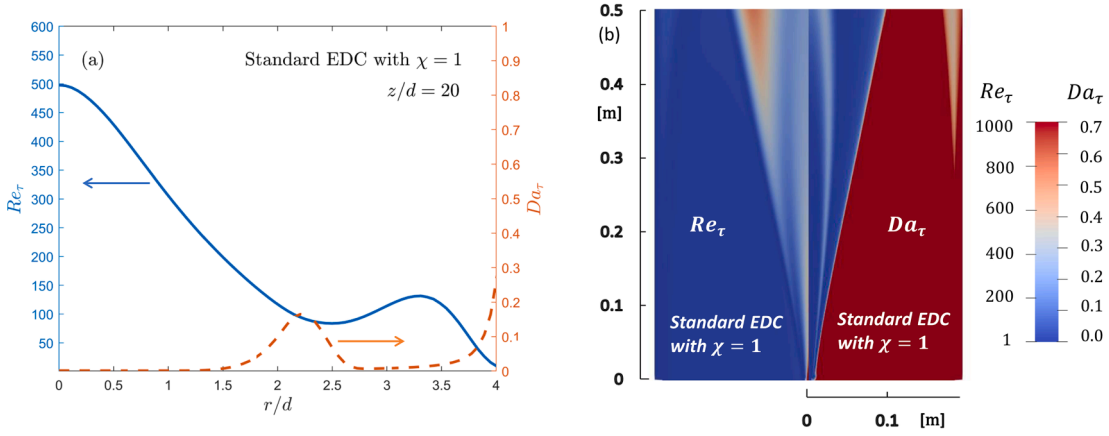

Fig. 4. (a) Radial profiles of Re_τ and Da_τ of simulated DLR-A at $z/d = 20$. (b) Re_τ and Da_τ fields from the same flame. Standard EDC with $\chi = 1$ was applied for all results.

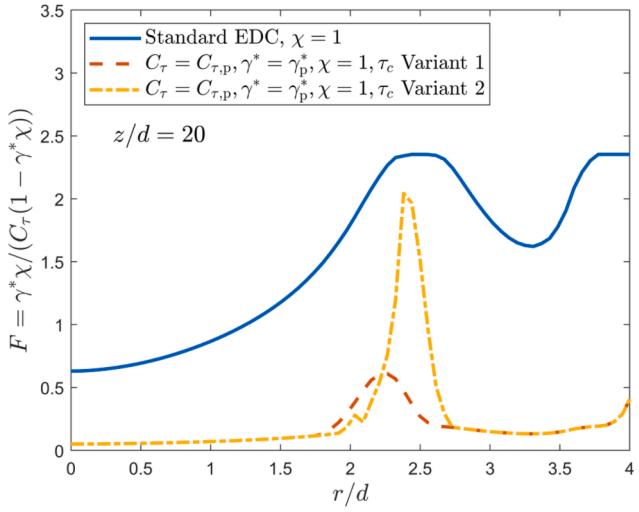

Fig. 5. Profiles of EDC Factor F obtained from v2020 EDC with τ_c Variant 1 (Eq. (8)), Variant 2 (Eq. (9)) and the standard EDC at $z/d = 20$. $\chi = 1$ for all cases.

Variant 1 showed a significant difference compared to the value from the standard EDC, meaning that the v2020 EDC would considerably reduce the overall reaction rate. On the contrary, Variant 2 showed little difference from the standard model near its peak value. It can be argued that the presence of hydrogen reaction, which is relatively fast, could contribute to the difference between the two variants. Unlike Variant 1, which only considers the methane reaction, Variant 2 considers all species formation rates. Nevertheless, outside the reaction zone, both variants similarly showed that F drops to almost nothing due to a very low Da_τ.

5. Constraints on γ_λ

5.1. Background

Theoretically, γ_λ is a major factor in the overprediction of $\overline{R}_k$ at low Re_τ. Lewandowski et al. [4] used $\gamma_{\lambda,\max} = 0.7$ for the studied cases with v2020 EDC (M. Lewandowski, personal communication, Jan.-Feb. 2021). However, an analysis was lacking regarding how much the accuracy of the model relied on the selected $\gamma_{\lambda,\max}$. This analysis might be crucial because it was figured out that the limiter could largely influence the simulation results [42]. Therefore, this section will demonstrate a sensitivity analysis of $\gamma_{\lambda,\max}$ to, specifically, the calculation of χ and $\overline{R}_k$.

5.2. The Adelaide flames, HM1 and HM3

The fine structure region mass fraction γ_λ appears in Eq. (5) for the calculation of χ. However, the previous studies [4,42] disregarded the maximum limit of γ_λ with the purpose of enhancing the reduction effect at $Re_\tau < 27.8$. Therefore, the impact of $\gamma_{\lambda,\max}$ on χ will be studied here.

A theoretical analysis can be made by plotting χ against Re_τ when $\gamma_{\lambda,\max}$ is set to 0.7, 0.95 and unlimited, as demonstrated in Fig. 6. For this,

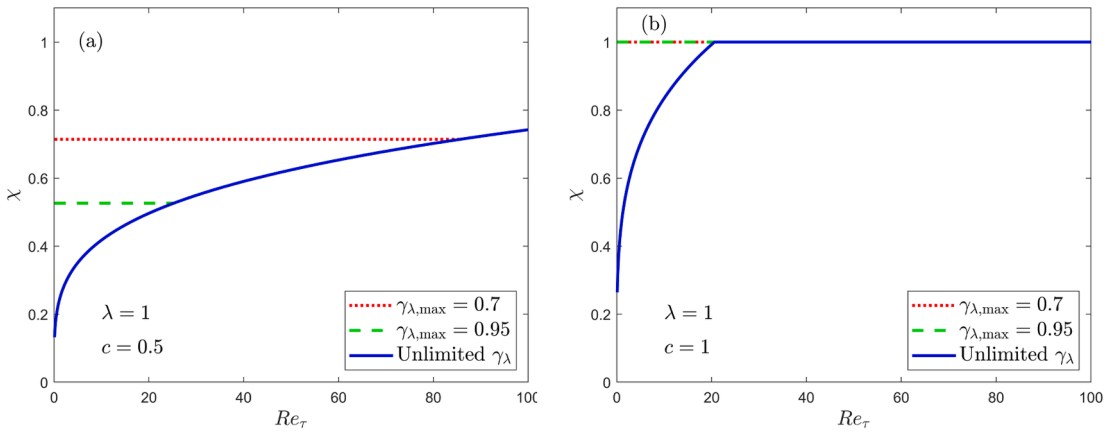

Fig. 6. Reacting fraction χ plotted against Re_τ (Eq. (5)) for three different $\gamma_{\lambda,\max}$: 0.7, 0.95 and unlimited. (a) Reaction progress $c = 0.5$ and (b) 1.0. Air excess ratio $\lambda = 1$ for all cases.

the air excess ratio (λ) was assumed to be constant at unity, and two different quantities of the reaction progress (c) were examined. The analysis showed that χ was sensitive to $\gamma_{\lambda,\max}$ when $c = 0.5$. Different profiles of χ can be generated depending on $\gamma_{\lambda,\max}$. However, at $c = 1$, $\chi = 1$ were obtained for both $\gamma_{\lambda,\max} = 0.7$ and 0.95. These results indicated that applying γ_λ without limit would maximalize the reduction of χ at low Re_τ.

Next, a comparison can be made by looking at the χ radial profiles obtained from the case of limited and unlimited $\gamma_{\lambda,\max}$. The former case refers to $\gamma_{\lambda,\max} = 0.95$. It is seen in Fig. 7 that the difference between the two cases is evident at $z = 60$ mm for both HM1 and HM3. This result can be explained by the fact that Re_τ was low near the nozzle. On the other hand, the χ profiles at an axial distance greater than 120 mm showed almost no difference as χ_2 and χ_3 were recorded to be unity.

Simulations with two different values of $\gamma_{\lambda,\max}$ were made using the v2020 EDC. It can be observed in Fig. 8 that increasing $\gamma_{\lambda,\max}$ from 0.7 to 0.95 resulted in temperature overprediction, particularly at $z = 120$ mm. This trend was followed by a decrease in Re_τ. It was found that the drop in Re_τ (see Fig. 8b) was sufficient to switch the model into using the standard EDC for predicting the reaction rate. The setting of $\gamma_{\lambda,\max}$ affected the Re_τ prediction because the temperature influenced kinematic viscosity.

5.3. The Delft flame, DJHC-I 4100

The v2020 EDC with $\chi = 1$ will be used in this section. It was reported [4] that this configuration had reduced $\overline{R}_k$ excessively in DJHC-I 4100. Accordingly, this section aims to investigate to what degree this result relies on the determination of $\gamma_{\lambda,\max}$. The ignition model will be absent ($Da_{\tau,\min} = 0$) to isolate the effect of $\gamma_{\lambda,\max}$.

Two different values of $\gamma_{\lambda,\max}$ were studied, i.e., 0.7 and 0.95. An interesting finding was the radial temperature profile at 120 mm from the nozzle exit, as depicted in Fig. 9a. At this location, the model was found sensitive to $\gamma_{\lambda,\max}$. The first case ($\gamma_{\lambda,\max} = 0.95$) in the figure shows a highly overpredicted temperature peak, while the second case ($\gamma_{\lambda,\max} = 0.7$) shows almost no peak. The result of the second case may explain the previous simulation [4], which reported extinction at the same location. To visualize the overall impact of $\gamma_{\lambda,\max}$, Fig. 9b shows the temperature field. The similarity between the two cases in the figure is that the flame seems to be extinguished near the nozzle due to the reduced reaction rate by the modified EDC constants. However, reactions start to occur further downstream. Furthermore, it can be observed that the case of $\gamma_{\lambda,\max} = 0.95$ has a higher maximum flame temperature.

The reduction effect on the reaction rate was maximized by assuming that $Da_{\tau,\min} = 0$. Nonetheless, the model could sustain the flame at a steady state. A possible explanation for this result is that a part of the flame did not fall under the MILD regime. To support this argument, Re_τ and Da_τ radial profiles at the exact location are presented in Fig. 10. The case of $\gamma_{\lambda,\max} = 0.95$ shows that the first Da_τ peak from the jet centre takes place due to the primary reaction zone. Interestingly, the absolute value of this peak is above unity, which may indicate that the flame is no longer "slow". Therefore, the reaction rate remained high (unmodified). In addition, the second peak in the figure occurs due to the non-uniform

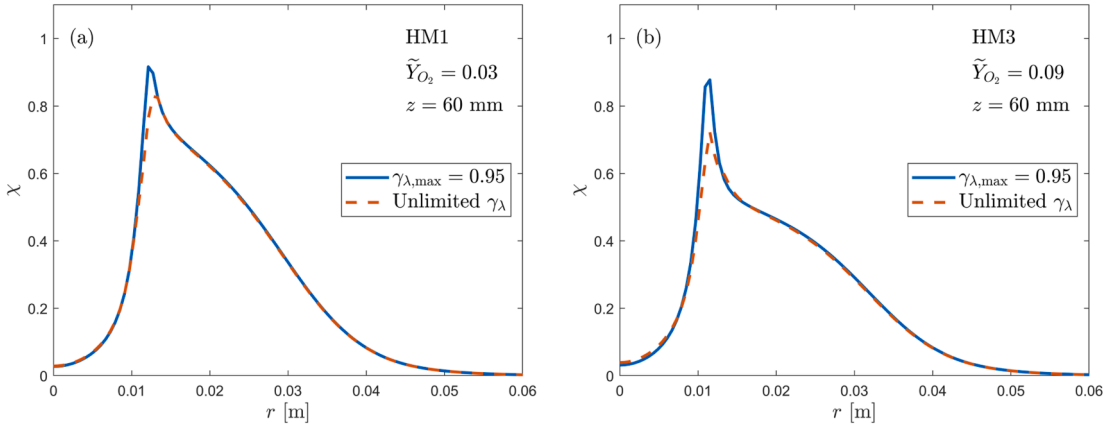

Fig. 7. Radial χ profiles obtained by post-processing the result of (a) HM1 and (b) HM3 using the standard EDC. Comparisons between γ_λ unlimited and limited ($\gamma_{\lambda,\max} = 0.95$). $z = 60$ mm for all cases.

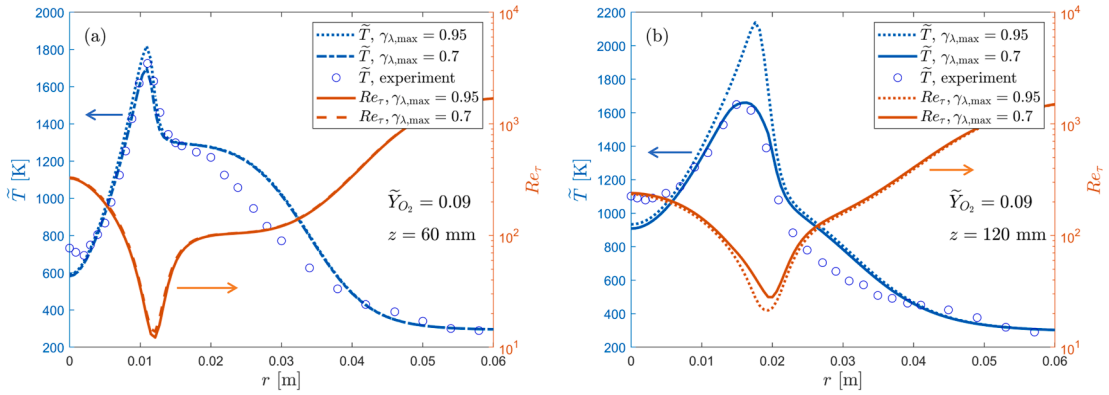

Fig. 8. (a) Radial profiles of temperature and Re_τ at (a) $z = 60$ and (b) 120 mm of HM3 using the v2020 EDC. Cases with $\gamma_{\lambda,max} = 0.95$ and 0.7 are compared to experimental data [12].

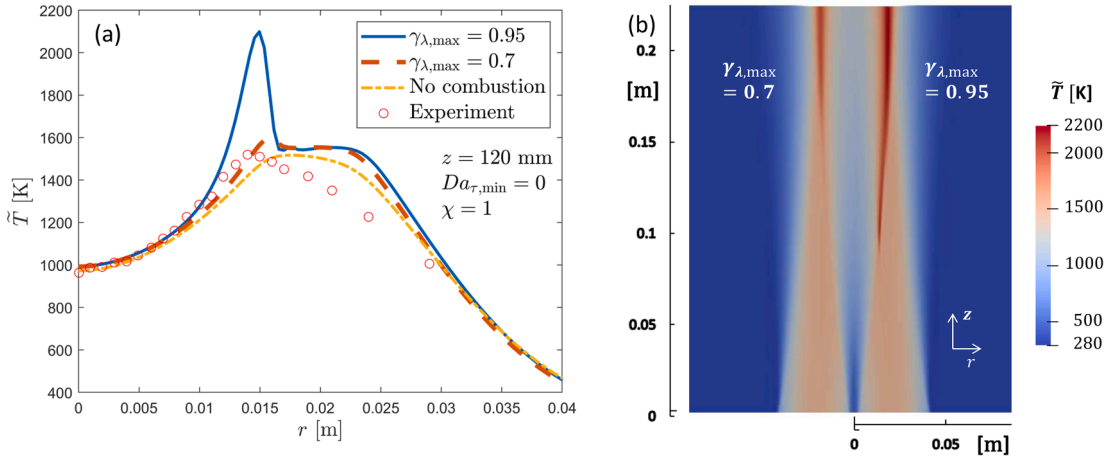

Fig. 9. (a) Radial plots of temperature at $z = 120$ mm of simulated DJHC-I 4100 using v2020 EDC with $\chi = 1$ and $Da_{\tau,\min} = 0$. Cases with $\gamma_{\lambda,\max} = 0.95$ and 0.7, no combustion (reaction switched off) and the experimental data [13] are compared. (b) Comparison of temperature fields when $\gamma_{\lambda,\max} = 0.7$ and 0.95.

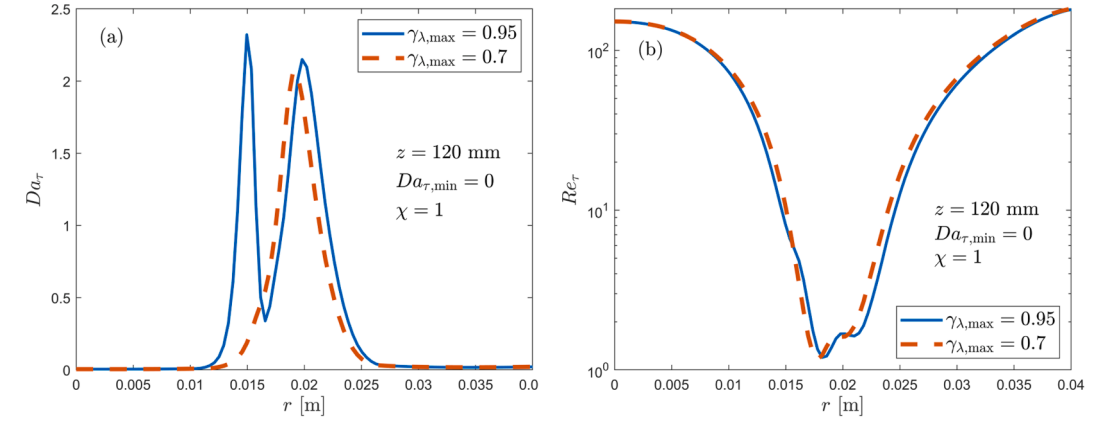

Fig. 10. Radial profiles of (a) Da_τ and (b) Re_τ at $z = 120$ mm of simulated DJHC-I 4100 using v2020 EDC with $Da_{\tau,\min} = 0$ and $\chi = 1$ for all cases. Comparison of two $\gamma_{\lambda,\max}$ values: 0.95 and 0.7.

boundary condition of the hot coflow. The same reasoning can be made to explain the presence of a similar Da_τ peak in the case of $\gamma_{\lambda,\max} = 0.7$. In contrast to the Da_τ profiles, the Re_τ profiles from both $\gamma_{\lambda,\max}$ cases do not show big differences. This was because they were affected mainly by the coflow. However, Re_τ drops almost to unity in the reaction zone ($15 < r < 25$ mm), indicating that the viscous forces are significant. Lastly, it should be remarked that the ability to sustain the flame without the ignition model does not mean that the ignition model was not necessary for igniting the flame at the beginning of the iterations.

5.4. Analysis using the EDC factor F

The EDC factor F, Eq. (6), can be utilized to analyse the impact of $\gamma_{\lambda,\max}$ in the standard EDC with $\chi = 1$. For example, it is shown in Fig. 11

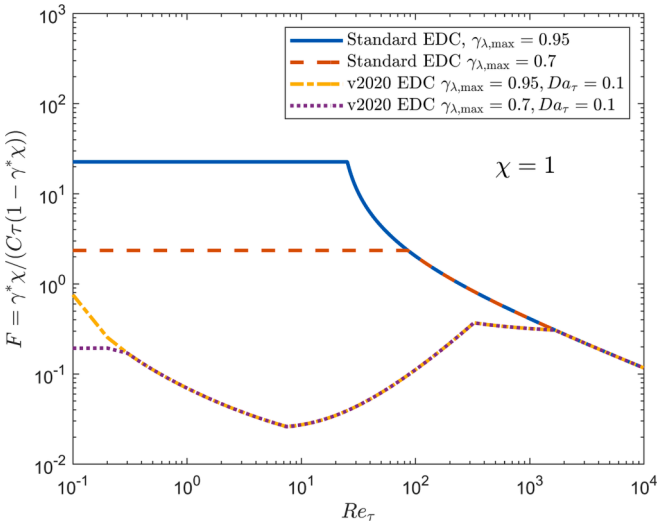

Fig. 11. Plots of EDC factor (F) against Re_τ obtained from standard and v2020 EDC. Two variants of $\gamma_{\lambda,\max}$ were studied: 0.95 and 0.7. For v2020 EDC, $Da_\tau = 0.1$ is chosen to enhance the effect of slow chemistry. The ignition model is neglected, and $\chi = 1$ is used for all cases.

that a decrease of $\gamma_{\lambda,\max}$ from 0.95 to 0.7 would reduce the maximum F by almost one order of magnitude. The considerable impact may indicate that flame extinguishment can take place merely due to clipping γ_λ, that is, without any sophisticated treatments on the EDC model constants. Analytically, F increases exponentially as Re_τ decreases, until reaching its peak value at $\gamma_\lambda = \gamma_{\lambda,\max}$. The peak value can be infinity if $\gamma_{\lambda,\max} = 1$, which means that $\overline{R}_k$ can also go to infinity (as long as there are reactants). It should be noted that the analysis using F is only meaningful if the effect of modifying the EDC model constants on τ^* is negligible.

When applying the v2020 EDC with $\chi = 1$, F will be small at low Re_τ and low Da_τ. For instance, at $Da_\tau = 0.1$ and $1 < Re_\tau < 1000$, F becomes smaller than the value from the standard EDC with $\chi = 1$. This effect was expected because, in the v2020 EDC, F becomes a function of the variables $C_{\gamma,p}$ and $C_{\tau,p}$. At high Re_τ, the F value obtained from both the v2020 EDC and the standard EDC with $\chi = 1$ will converge as $C_{\gamma,p}$ and $C_{\tau,p}$ approach their standard values. More interestingly, the effect of reducing $\gamma_{\lambda,\max}$ from 0.95 to 0.7 is less significant for the v2020 EDC. F from both $\gamma_{\lambda,\max}$ cases are identical except when $Re_\tau < 1$. Furthermore, the F profile shows discontinuities due to the limiters on $C_{\gamma,p}$ and $C_{\tau,p}$. F starts to increase again at a $Re_\tau < 10$, which is undesirable. This effect may indicate that the model has a limited range of validity. A more detailed theoretical review was given by Ertesvåg [47].

6. Constraints on Da_τ

6.1. Background

A sensitivity analysis will be carried out on the minimum limit of Da_τ (the ignition model). Section 4 has investigated the significance of the proposed ignition model. This section will reveal to what degree the simulation results would change when tuning the Da_τ limiter. For this purpose, different constant values of $Da_{\tau,\min}$ will be tested against HM1. This investigation might also be helpful in the context of DJHC-I 4100 since the ignition model failed to maintain the reaction when applying v2020 EDC with $\chi = 1$ [4]. In addition, a similar investigation will be conducted for DLR-A. It should be noted that the values of $Da_{\tau,\min}$ in the following sensitivity studies were chosen arbitrarily to explore the potential (maximum and minimum) effect of introducing the ignition model.

6.2. The Adelaide flame, HM1

Three different values were analysed for $Da_{\tau,\min}$: 0.3, 0.03 and 0.003, and the comparison of these cases is given in Fig. 12. Here, $\gamma_{\lambda,\max} = 0.95$ was used to discard/minimize the reduction of reaction rate due to clipping $\gamma_{\lambda,\max}$ far below unity. It was found that tuning $Da_{\tau,\min}$ to 0.3 almost nullified the slow chemistry/extinction effect obtained from the locally modified constants. On the other hand, a value of $Da_{\tau,\min}$ down to 0.003 led to almost full extinction. The minimum limit of Da_τ became a decisive parameter for obtaining good accuracy. In the case of $Da_{\tau,\min} = 0.03$, the temperature and CO_2 mass fraction profile agreed relatively well with the experimental values. This result was, however, followed by an overshooting of the OH mass fraction. The previous study [4] also found this issue. The determination of $Da_{\tau,\min}$ was responsible for the distribution of the volumetric reaction heat release rate ($\dot{Q}/V$). Two peaks (denoted as the primary and secondary reaction in Section 4.2) are visible in Fig. 12d when setting $Da_{\tau,\min} = 0.03$. The gap between the two peaks was present due to less reactions as $0 > Da_\tau > Da_{\tau,\min}$ (cf. Fig. 2c for an illustration from the variable $Da_{\tau,\min}$). This gap became smaller when moving upstream, and the two edges eventually merged when $Re_\tau < Re_{\tau,\text{limit}}$. When the standard EDC model takes the role, the variable χ in Eq. (5) only allows the reaction rate to maximize at stoichiometric mixture fraction. In addition, it was found that decreasing $Da_{\tau,\min}$ below 0.03 would eliminate the inner peak without combining with the outer peak.

6.3. The Delft flame, DJHC-I 4100

The v2020 EDC with $\chi = 1$ was used while keeping $\gamma_{\lambda,\max} = 0.7$. Three different constant values were selected for $Da_{\tau,\min}$: 1.0, 0.1 and 0.01. Radial temperature profiles for two axial locations (60 mm and 120 mm from the nozzle) are presented in Fig. 13. A considerable decrease in the temperature spike is visible when reducing $Da_{\tau,\min}$ from 1 to 0.1. However, for $Da_{\tau,\min}$ lower than 0.1, the difference was minor. It can be argued that setting $Da_{\tau,\min} = 1$ may nullify any modification effects as the constants would revert to their standard values when the chemistry is no longer slow. However, the profile with $Da_{\tau,\min} = 1$ in the figure still shows a lower temperature peak compared to the result from the standard EDC with $\chi = 1$. A relatively high value of Da_τ might be responsible for this result. Generally, a similar temperature pattern could be seen at both axial locations. However, it is more evident that at $z = 120$ mm location, tuning the $Da_{\tau,\min}$ below 0.1 almost gave nearly no change in the temperature profile. This lack of impact is reasonable because Da_τ increased downstream.

6.4. The DLR-A flame

It could be interesting to analyse the effect of using different values of $Da_{\tau,\min}$ on DLR-A. This analysis is important considering the presence of "low" Re_τ and/or "low" Da_τ in the reaction zone, cf. Section 4.3 (for the Re_τ and Da_τ fields). It should be noted that the statement of "low" here is a subjective observation from the v2020 EDC point of view. Three different $Da_{\tau,\min}$ values were examined: 0.1, 0.01 and 0. The last case was meant to observe the maximum reduction effect on the temperature/reaction rate. $\chi = 1$ was assumed to avoid a lifting flame.

The radial temperature profiles at the axial location of 20d are presented in Fig. 14 to analyse the effects of using two different variants of τ_c in the v2020 EDC, cf. Section 2.2 for the definition of the variants. For Variant 1, it was revealed that the flame could be affected considerably by the locally modified EDC constants. The role of the ignition model, in this case, was critical because the absence of an ignition model ($Da_{\tau,\min} = 0$) resulted in total extinction. Setting $Da_{\tau,\min}$ up to 0.1 could adjust the temperature peak to a higher level. This effect was similarly observed in DJHC-I 4100, cf. Section 6.3. For Variant 2, the temperature reduction effect had become minor. This result was expected due to the

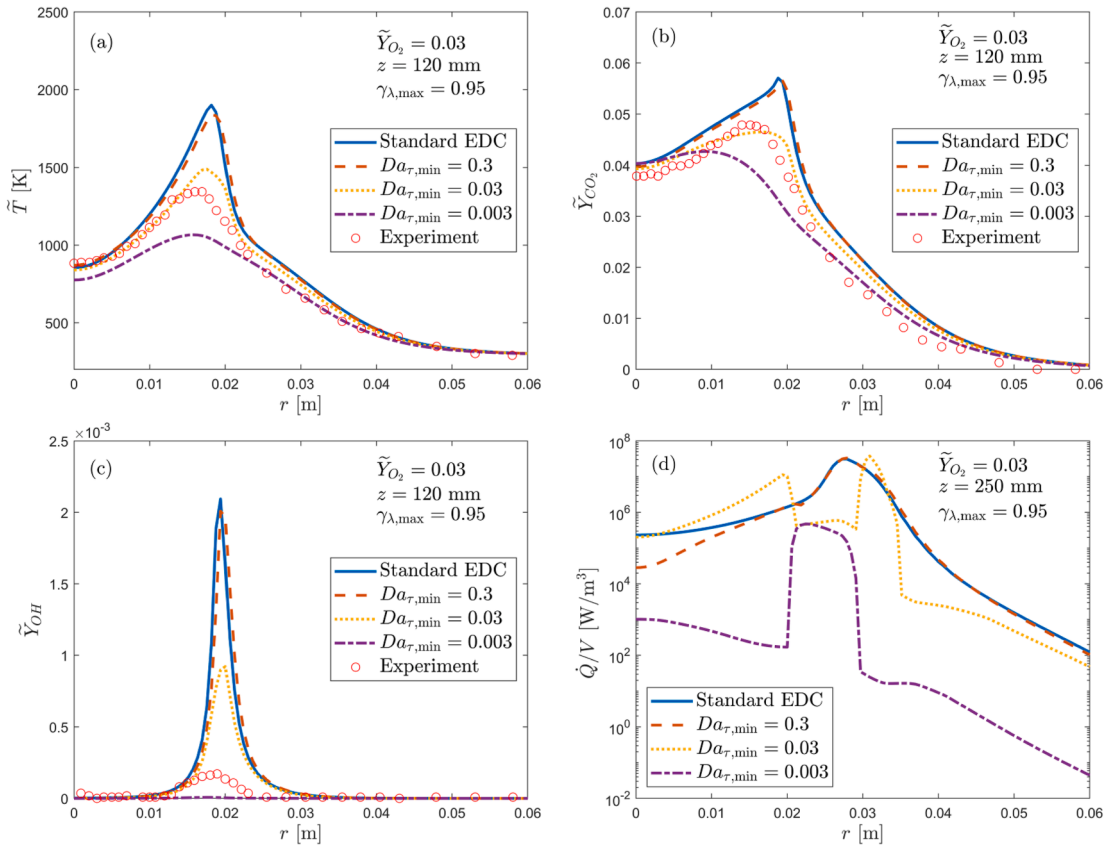

Fig. 12. Radial plots of (a) temperature, (b) CO_2 mass fraction, (c) OH mass fraction, and (d) volumetric reaction heat release rate of simulated HM1. Results of standard EDC, v2020 EDC with three different $Da_{\tau,\min}$ values and experimental data [12] are compared. $\gamma_{\lambda,\max} = 0.95$ for all cases.

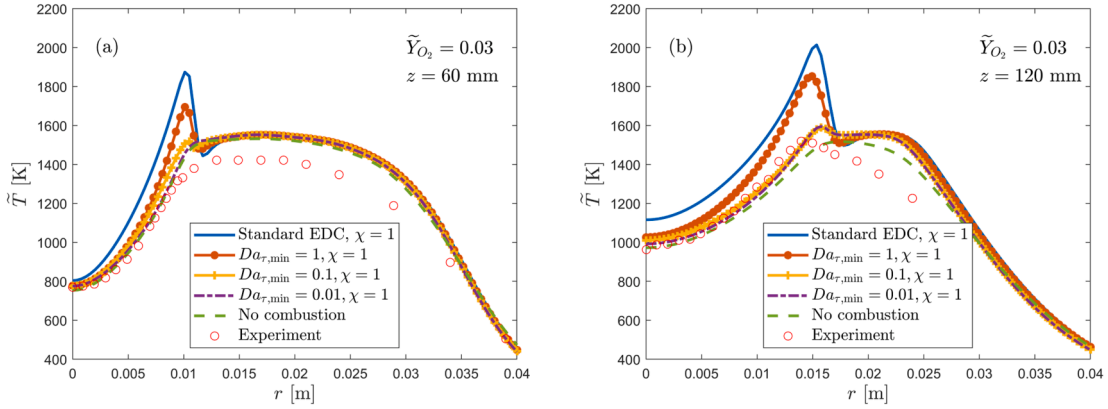

Fig. 13. Radial temperature profiles at (a) $z = 60$ and (b) 120 mm of simulated DJHC-I 4100 flame using the v2020 EDC. Results of standard EDC with, v2020 EDC with three different $Da_{\tau,\min}$ values and experimental data [13] are compared. $\chi = 1$ for reacting cases.

higher Da_τ and F, compared to those from Variant 1, cf. Section 4.3 for more analyses on Da_τ and F.

It is important to note that the overprediction of the peak temperature did not necessarily represent the same problem as that of the MILD flames. This issue was considered out of scope in the present study.

7. The effect of the turbulence model

A switch mechanism was introduced in Eq. (11) at $Re_\tau = 27.8$ (limit). A significant temperature gradient may take place near the limit, as shown in Fig. 1. Therefore, the overall accuracy of the v2020 EDC can be dependent on the performance of the turbulence model in predicting the location of the limit. The use of different variants of $k-\varepsilon$ model was investigated previously [42], however with the purpose of improving the prediction of the jet spreading rate for MILD flames. Accordingly, this section will investigate the effect of varying turbulence models on the Re_τ prediction.

Different two-equation turbulence models were examined: Pope $k-\varepsilon$, standard $k-\varepsilon$ (i.e., with $C_{\varepsilon 1} = 1.44$), standard $k-\varepsilon$ with modified $C_{\varepsilon 1} = 1.6$, realizable $k-\varepsilon$ and $k-\omega$ SST. The impact of the turbulence models on the profiles of temperature and Re_τ of HM1 is depicted in Fig. 15. The profiles are shown radially at $z = 120$ and 200 mm to represent the reaction at $Re_\tau < 27.8$ and $Re_\tau > 27.8$ (termed as Zone 1 and 2 in Section 4.2), respectively. It should be pointed out that $\gamma_{\lambda,\max} = 0.95$ was used, which could contribute to overpredicting the overall temperature (cf. Section 5.2).

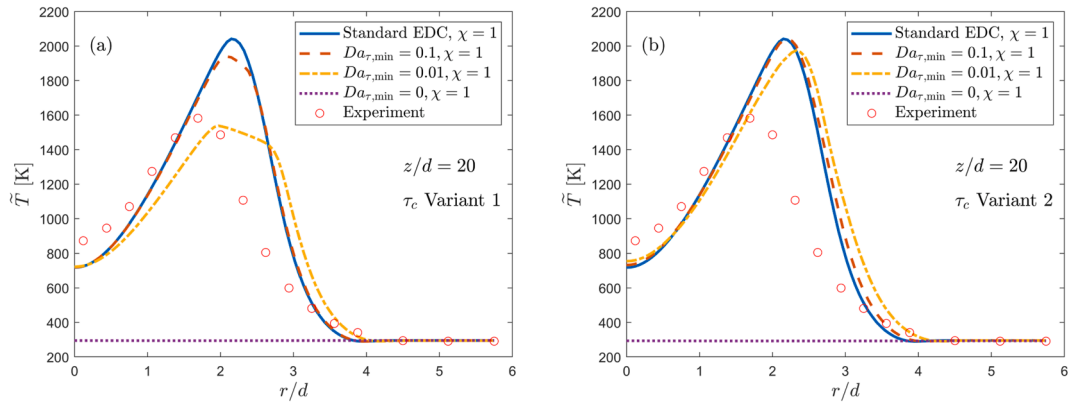

Fig. 14. Radial temperature profiles at $z = 20d$ of simulated DLR-A using the v2020 EDC and (a) Variant 1 of τ_c and (b) Variant 2. Results of standard EDC, v2020 EDC with three different $Da_{\tau,\min}$ values and experimental data [55] are compared. $\chi = 1$ for all cases.

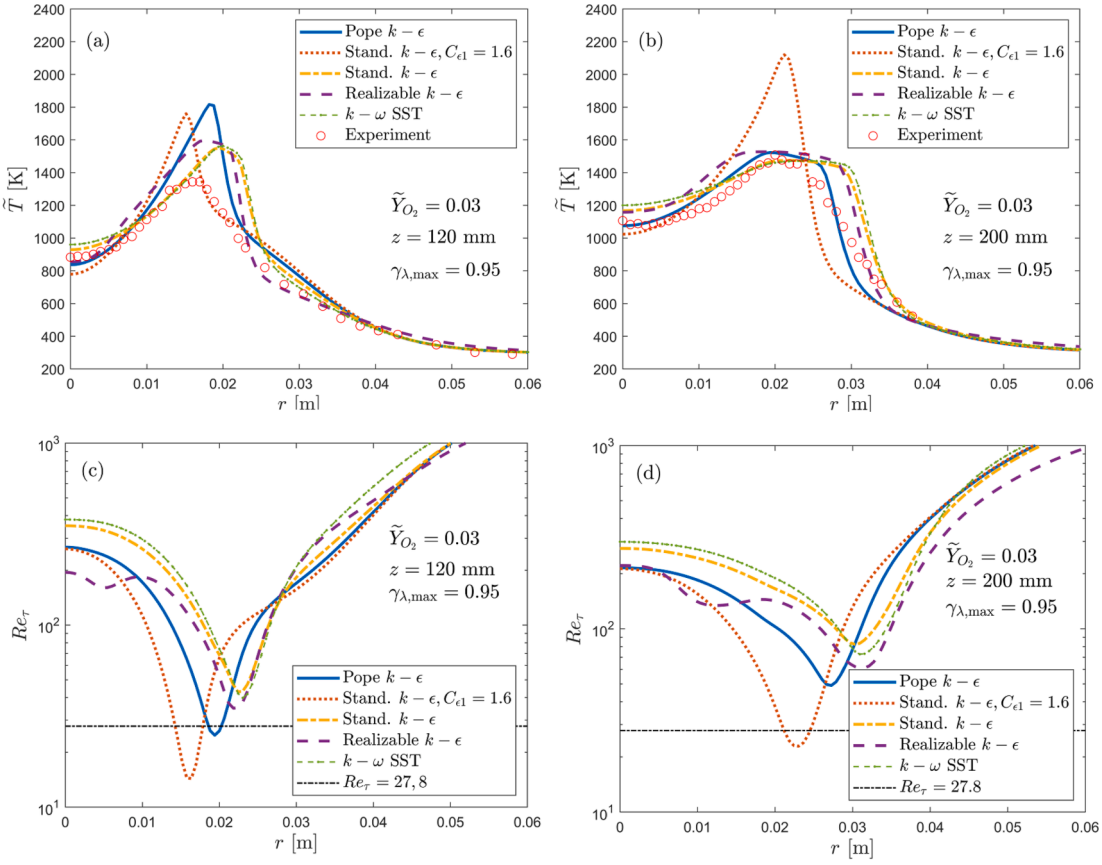

Fig. 15. Radial profiles of temperatures (a,b) and Re_τ (c,d) at $z = 120$ mm (a,c) and $z = 200$ mm (b,d) of simulated HM1 using the v2020 EDC with $\gamma_{\lambda,\max} = 0.95$. Comparison of different turbulence models together with experimental data [12].

The standard $k-\varepsilon$ model was proven to work reasonably well in previous studies [24,26]. However, in the present work, the model significantly overpredicted the temperature of HM1 at $z = 200$ mm. The modification of $C_{\varepsilon 1}$ (from 1.44 to 1.6) gave a larger additional production of ε, compared to the Pope $k-\varepsilon$. An increase in ε resulted in a decrease in Re_τ to a level below 27.8 in the reaction zone. Under this condition, $\overline{R}_k$ was solved by using Eq. (4), which eventually led to temperature overprediction. At $z = 120$ mm, both Pope $k-\varepsilon$ and standard $k-\varepsilon$ allowed Re_τ to drop below the limit, thus resulting in a higher temperature peak compared to the remaining models.

The standard $k-\varepsilon$ model also made a contrast in the profiles of Da_τ and F at $z = 200$ mm, as shown in Fig. 16. A high temperature peak increased the kinetics of the reactions, thus raising Da_τ. The F profile follows a similar pattern in which the highest spike was evident for the second model due to the use of the standard EDC. On the contrary, the other models show low spikes of F, which are attributed to the ignition model (applying the standard EDC when $Da_\tau < Da_{\tau,\min}$). It could be observed that F could drop to zero before increasing again at a larger radius. This drop occurred due to the extinction effect by the locally modified EDC constants.

8. Overall discussion

The ignition model has increased the sensitivity of EDC. Different

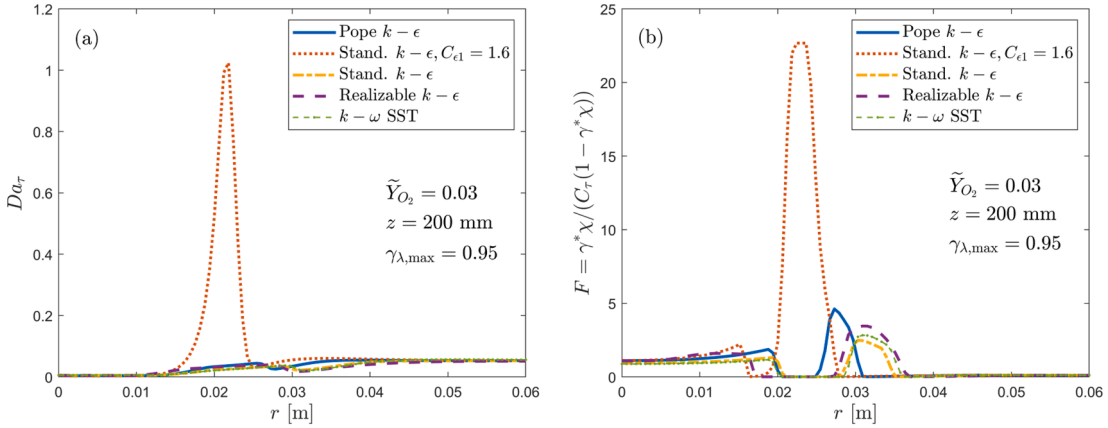

Fig. 16. Radial profiles of (a) Da_τ and (b) F at $z = 120$ mm of simulated HM1 using the v2020 EDC with $\gamma_{\lambda,\max} = 0.95$. Comparison of different turbulence models.

methods for the calculation of τ_c could impact the simulation results significantly, not only for MILD flames but also for conventional flames. It can be argued that different values or expressions for $Da_{\tau,\min}$ might be necessary to improve the generality while maintaining the overall accuracy of the model. The current expression of τ_c also leaves some issues. For instance, $C_{\tau,p}$ was not added in the expression of the mixing time scale τ_η, which made τ_η higher than τ^*. Moreover, the selected τ_c in the v2020 EDC was a function of temperature only. Therefore, the physicality of $Da_\tau \gg 1$ was questionable for non-reacting hot gas. An example of alternatives would be to estimate Da_τ based on the heat transfer rate [40] or scalar dissipation rate [60]. Another possibility is to estimate Da_τ from the fine structure quantities, e.g., $Da_\tau = R_k^*\tau^*/\rho^*$, cf. Eq. (9) .

The limitation on γ_λ played a major factor in the accuracy of the model. However, the limitation method still requires a fundamental justification concerning the fine structure reactor model. The reactor mass balance needs to be revisited in weakly turbulent flames. When γ_λ approaches unity, the surrounding region would be limited/absent. A possible treatment under such a condition is to apply a batch reactor model with the initial condition obtained from the mean quantities. By doing so, a numerical advantage can also be achieved because the appearance of $(1-\chi\gamma_\lambda{}^n)$ as a denominator in the overall mass balance equation can be avoided. Furthermore, a batch reactor model allows "slow reactions" at a reactor level. This capability is an advantage over the adiabatic PSR model, in which incomplete reactions (not extinction) may violate heat and mass conservation [61].

A future step would be to introduce modifications that are supported by analysis of the currently existing model. The next development of EDC should be able to explain the transition towards the laminar combustion model conceptually. When Re_τ is very low, any expressions based on turbulence quantities may no longer be representative. For example, the current τ_η is inversely proportional to $\sqrt{\varepsilon}$, so that its validity at very low ε should be addressed. On the contrary, the reactor residence time is estimated from the diffusion/convection time scale when it comes to the laminar combustion model.

9. Concluding remarks

Analyses have been made to understand the significance of the ignition model and key limiters, i.e., the maximum fine structure mass fraction ($\gamma_{\lambda,\max}$), the minimum Damköhler number ($Da_{\tau,\min}$) and the minimum local turbulence Reynolds number ($Re_{\tau,\text{limit}}$) for restricting the use of the extended EDC (v2020) in capturing the effect of slow chemistry and low turbulence. The limiters were responsible for achieving the reported accuracy in the context of RANS.

The reversion of the EDC model constants at $Da_\tau < Da_{\tau,\min}$ is found critical not only to enable the ignition but also to distribute reactions. It is found that the ignition model enables reactions close to the jet centre (secondary reactions) of the Adelaide HM1 flame. The selection of of $Da_{\tau,\min}$ is also decisive for the accuracy of the model. The sensitivity study shows that a high threshold ($Da_{\tau,\min} > 0.3$) can cancel the reduction effect on $\overline{R}_k$, whereas a low threshold ($Da_{\tau,\min} < 0.03$) can result in complete extinction. A similar effect of $Da_{\tau,\min}$ is also observed in the Delft DJHC-I 4100 flame.

The investigation against the DLR-A flame shows that the v2020 EDC underpredict the Da_τ field. Consequently, the overall reaction rate is modified similarly to that of MILD flames. The estimation method for τ_c plays an important role in the simulations. It is found that calculating τ_c based on the local formation rate can dramatically change the prediction of Da_τ as well as the temperature profiles.

The introduction of $\gamma_{\lambda,\max}$ in the formulation of χ_2 and χ_3 of the reaction fraction can decrease the maximum χ value in the reaction zone, e.g., in the Adeleide HM1 and HM3 flames. More importantly, the determination of $\gamma_{\lambda,\max}$ is influential for the prediction of other variables. Hypothetically, an increase in $\gamma_{\lambda,\max}$ would raise the maximum flame temperature, and the temperature affects Re_τ and Da_τ fields. The present work demonstrates that an increase of $\gamma_{\lambda,\max}$ from 0.7 to 0.95 significantly impacted the Re_τ field of HM3, thus resulting in temperature overprediction at some locations of the flame. A similar sensitivity study performed for DJHC-I 4100 (with $\chi = 1$) shows that $\gamma_{\lambda,\max} = 0.95$ can change the Da_τ profile such that Da_τ is larger than unity near the reaction zone.

The hybrid mechanism in the v2020 EDC has split reactions in HM1 into two different zones, indicating different EDC formulations for calculating the mean reaction rate. The location of the limit between the two zones is dependent on the prediction of Re_τ. An increase of $\gamma_{\lambda,\max}$ from 0.7 to 0.95 has substantially shifted the limit for HM3. Moreover, the use of the $k-\varepsilon$ turbulence model with modified $C_{\varepsilon 1}$ resulted in significantly higher downstream temperature profiles compared to those from the other $k-\varepsilon$ variants.

CRediT authorship contribution statement

Bima A. Putra: Conceptualization, Methodology, Validation, Formal analysis, Visualization, Writing – original draft, Writing – review & editing. **Ivar S. Ertesvåg:** Conceptualization, Methodology, Supervision, Writing – review & editing.

Declaration of Competing Interest

The authors declare that they have no known competing financial interests or personal relationships that could have appeared to influence the work reported in this paper.

Data availability

Data will be made available on request.

Acknowledgements

The authors thank Michal T. Lewandowski (researcher at NTNU) for sharing valuable information regarding the OpenFOAM model settings from his previous works.

The authors gratefully acknowledge the financial support by the Research Council of Norway and several partners through the Fire Research and Innovation Centre (www.fric.no). Research Council of Norway, programme BRANNSIKKERHET, project number 294649.

References

[1] Magnussen BF. Modeling of NOx and soot formation by the eddy dissipation concept. Int. Flame Res. Found. 1st Top. oriented Tech. Meet., Amsterdam, Holland: 17-19 Oct 1989.
[2] Magnussen BF. On the structure of turbulence and generalized Eddy Dissipation Concept for chemical reaction in turbulent flow. 19th Am Inst Aeronaut Astronaut Aerosp Sci Meet, StLouis, Missouri 1981.
[3] Lewandowski MT, Parente A, Pozorski J. Generalised Eddy Dissipation Concept for MILD combustion regime at low local Reynolds and Damköhler numbers. Part 1: Model framework development. Fuel 2020;278:117743.
[4] Lewandowski MT, Li Z, Parente A, Pozorski J. Generalised Eddy Dissipation Concept for MILD combustion regime at low local Reynolds and Damköhler numbers. Part 2: Validation of the model. Fuel 2020;278:117773.
[5] Romero-Anton N, Huang X, Bao H, Martin-Eskudero K, Salazar-Herran E, Roekaerts D. New extended eddy dissipation concept model for flameless combustion in furnaces. Combust Flame 2020;220:49–62. https://doi.org/10.1016/j.combustflame.2020.06.025.
[6] He D, Yu Y, Kuang Y, Wang C. Analysis of EDC constants for predictions of methane MILD combustion. Fuel 2022;324:124542. https://doi.org/10.1016/j.fuel.2022.124542.
[7] Huang M, Deng H, Liu Y, Zhang B, Cheng S, Zhang X, et al. Effect of fuel type on the MILD combustion of syngas. Fuel 2020;281:118509.
[8] Zhou S, Zhu X, Yan B, Gao Q, Chen G, Li B. Role of a hot coflow on establishment of MILD combustion of biomass gasified gas. Fuel 2022;314:123142. https://doi.org/10.1016/j.fuel.2022.123142.
[9] Szegö GG, Dally BB, Nathan GJ. Scaling of NOx emissions from a laboratory-scale mild combustion furnace. Combust Flame 2008;154:281–95. https://doi.org/10.1016/j.combustflame.2008.02.001.
[10] Cano Ardila FE, Obando Arbeláez JE, Amell Arrieta AA. Emissions and dynamic stability of the flameless combustion regime using hydrogen blends with natural gas. Int J Hydrogen Energy 2021;46:1246–58. https://doi.org/10.1016/j.ijhydene.2020.09.236.
[11] Weber R, Gupta AK, Mochida S. High temperature air combustion (HiTAC): How it all started for applications in industrial furnaces and future prospects. Appl Energy 2020;278:115551. https://doi.org/10.1016/j.apenergy.2020.115551.
[12] Dally BB, Karpetis AN, Barlow RS. Structure of turbulent non-premixed jet flames in a diluted hot coflow. Proc Combust Inst 2002;29:1147–54. https://doi.org/10.1016/S1540-7489(02)80145-6.
[13] Oldenhof E, Tummers MJ, van Veen EH, Roekaerts DJEM. Role of entrainment in the stabilisation of jet-in-hot-coflow flames. Combust Flame 2011;158:1553–63. https://doi.org/10.1016/j.combustflame.2010.12.018.
[14] Huang X. Measurements and model development for flameless combustion in a lab-scale furnace 2018. https://doi.org/10.4233/uuid.
[15] Xu S, Tu Y, Huang Pu, Luan C, Wang Z, Shi B, et al. Effects of wall temperature on methane MILD combustion and heat transfer behaviors with non-preheated air. Appl Therm Eng 2020;174:115282.
[16] Khoshhal A, Rahimi M, Alsairafi AA. CFD study on influence of fuel temperature on NOx emission in a HiTAC furnace. Int Commun Heat Mass Transf 2011;38:1421–7. https://doi.org/10.1016/j.icheatmasstransfer.2011.08.008.
[17] Fortunato V, Giraldo A, Rouabah M, Nacereddine R, Delanaye M, Parente A. Experimental and numerical investigation of a MILD combustion chamber for micro gas turbine applications. Energies 2018;11:3363. https://doi.org/10.3390/en11123363.
[18] Cheong K-P, Wang G, Mi J, Wang B, Zhu R, Ren W. Premixed MILD combustion of propane in a cylindrical furnace with a single jet burner: combustion and emission characteristics. Energy Fuel 2018;32:8817–29. https://doi.org/10.1021/acs.energyfuels.8b01587.
[19] Buczyński R, Uryga-Bugajska I, Tokarski M. Recent advances in low-gradient combustion modelling of hydrogen fuel blends. Fuel 2022;328:125265. https://doi.org/10.1016/j.fuel.2022.125265.
[20] Minamoto Y, Swaminathan N. Modelling paradigms for MILD combustion. Int J Adv Eng Sci Appl Math 2014;6:65–75. https://doi.org/10.1007/s12572-014-0106-x.
[21] Ertesvåg IS. Analysis of some recently proposed modifications to the eddy dissipation concept (EDC). Combust Sci Technol 2020;192(6):1108–36.
[22] Mansourian M, Kamali R. Modifying the constant coefficients of Eddy-dissipation concept model in moderate or intense low-oxygen dilution combustion using inverse problem methodology. Acta Astronaut 2019;162:546–54. https://doi.org/10.1016/j.actaastro.2019.07.002.
[23] Kuang Y, He B, Wang C, Tong W, He D. Numerical analyses of MILD and conventional combustions with the Eddy Dissipation Concept (EDC). Energy 2021;237:121622. https://doi.org/10.1016/j.energy.2021.121622.
[24] Parente A, Malik MR, Contino F, Cuoci A, Dally BB. Extension of the Eddy Dissipation Concept for turbulence/chemistry interactions to MILD combustion. Fuel 2016;163:98–111. https://doi.org/10.1016/j.fuel.2015.09.020.
[25] Minamoto Y, Swaminathan N, Cant RS, Leung T. Reaction zones and their structure in MILD combustion. Combust Sci Technol 2014;186:1075–96. https://doi.org/10.1080/00102202.2014.902814.
[26] Evans MJ, Petre C, Medwell PR, Parente A. Generalisation of the eddy-dissipation concept for jet flames with low turbulence and low Damköhler number. Proc Combust Inst 2019;37:4497–505. https://doi.org/10.1016/j.proci.2018.06.017.
[27] Romero-Anton N, Martin-Escudero K, Ren M, Azkorra-Larrinaga Z. Consideration of the interactions between the reaction zones in the new extended Eddy dissipation concept model. Comput Fluids 2022;233:105203. https://doi.org/10.1016/j.compfluid.2021.105203.
[28] Mardani A, Nazari A. Dynamic adjustment of the Eddy Dissipation Concept model for turbulent/combustion interactions in mixed combustion regimes. Combust Flame 2022;241:111873. https://doi.org/10.1016/j.combustflame.2021.111873.
[29] Li Z, Cuoci A, Sadiki A, Parente A. Comprehensive numerical study of the Adelaide Jet in Hot-Coflow burner by means of RANS and detailed chemistry. Energy 2017;139:555–70. https://doi.org/10.1016/j.energy.2017.07.132.
[30] Azarinia A, Mahdavy-Moghaddam H. Comprehensive numerical study of molecular diffusion effects and Eddy Dissipation Concept model in MILD combustion. Int J Hydrogen Energy 2021;46:9252–65. https://doi.org/10.1016/j.ijhydene.2020.12.206.
[31] Farokhi M, Birouk M. A new EDC approach for modeling turbulence/chemistry interaction of the gas-phase of biomass combustion. Fuel 2018;220:420–36. https://doi.org/10.1016/j.fuel.2018.01.125.
[32] Farokhi M, Birouk M. Assessment of fractal/wrinkling theories for describing turbulent reacting fine structures under MILD combustion regimes. Combust Sci Technol 2020;193:1798–825. https://doi.org/10.1080/00102202.2020.1715963.
[33] Schaffel N, Mancini M, Szlęk A, Weber R. Mathematical modeling of MILD combustion of pulverized coal. Combust Flame 2009;156:1771–84. https://doi.org/10.1016/j.combustflame.2009.04.008.
[34] Xu M, Tu Y, Zeng G, Yang W. Evaluation of ignition process and NOx reduction of coal under moderate and intensive low-oxygen dilution combustion by implementing fuel-rich/lean technology. Fuel 2021;296:120657. https://doi.org/10.1016/j.fuel.2021.120657.
[35] Cheong K-P, Li P, Wang F, Mi J. Emissions of NO and CO from counterflow combustion of CH4 under MILD and oxyfuel conditions. Energy 2017;124:652–64. https://doi.org/10.1016/j.energy.2017.02.083.
[36] Zhang Z, Li X, Zhang L, Luo C, Mao Z, Xu Y, et al. Numerical investigation of the effects of different injection parameters on Damköhler number in the natural gas MILD combustion. Fuel 2019;237:60–70.
[37] Ebrahimi Fordoei E, Mazaheri K. Effects of preheating temperature and dilution level of oxidizer, fuel composition and strain rate on NO emission characteristics in the syngas moderate or intense low oxygen dilution (MILD) combustion. Fuel 2021;285:119118. https://doi.org/10.1016/j.fuel.2020.119118.
[38] Maragkos G, Beji T, Merci B. Towards predictive simulations of gaseous pool fires. Proc Combust Inst 2019;37:3927–34. https://doi.org/10.1016/j.proci.2018.05.162.
[39] Dorofeev SB. Thermal quenching of mixed eddies in non-premixed flames. Proc Combust Inst 2017;36:2947–54. https://doi.org/10.1016/j.proci.2016.06.061.
[40] Ren N, Zeng D, Meredith KV, Wang Y, Dorofeev SB. Modeling of flame extinction/re-ignition in oxygen-reduced environments. Proc Combust Inst 2019;37:3951–8. https://doi.org/10.1016/j.proci.2018.06.076.
[41] Gran IR, Magnussen BF. A numerical study of a bulff-body stabilized diffusion flame. Part 2. Influence of combustion modeling and finite-rate chemistry. Combust Sci Technol 1996;119:191–217.
[42] Lewandowski MT, Ertesvåg IS. Analysis of the Eddy Dissipation Concept formulation for MILD combustion modelling. Fuel 2018;224:687–700. https://doi.org/10.1016/j.fuel.2018.03.110.
[43] Magnussen BF. The Eddy Dissipation Concept: A Bridge Between Science and Technology. ECCOMAS Themat. Conf. Comput. Combust., Lisbon: 21-24 June 2005.
[44] Ertesvåg IS, Magnussen BJØRNF. The eddy dissipation turbulence energy cascade model. Combust Sci Technol 2000;159(1):213–35.
[45] De A, Oldenhof E, Sathiah P, Roekaerts D. Numerical simulation of Delft-Jet-in-Hot-Coflow (DJHC) flames using the eddy dissipation concept model for turbulence-chemistry interaction. Flow, Turbul Combust 2011;87:537–67. https://doi.org/10.1007/s10494-011-9337-0.
[46] Snegirev AY. Perfectly stirred reactor model to evaluate extinction of diffusion flame. Combust Flame 2015;162:3622–31. https://doi.org/10.1016/j.combustflame.2015.06.019.
[47] Ertesvåg IS. Scrutinizing proposed extensions to the Eddy Dissipation Concept (EDC) at low turbulence Reynolds numbers and low Damköhler numbers. Fuel 2022;309:122032. https://doi.org/10.1016/j.fuel.2021.122032.
[48] Pope SB. An explanation of the turbulent round-jet/plane-jet anomaly. AIAA J 1978;16:279–81. https://doi.org/10.2514/3.7521.

[49] Shih TH, Liou WW, Shabbir A, Yang Z, Zhu J. A new k-ϵ eddy viscosity model for high reynolds number turbulent flows. Comput Fluids 1995;24:227–38. https://doi.org/10.1016/0045-7930(94)00032-T.
[50] Menter FR, Esch T. Elements of industrial heat transfer predictions. 16th Brazilian Congr Mech Eng 2001.
[51] Menter FR. Two-equation eddy-viscosity turbulence models for engineering applications. AIA A J 1994;32(8):1598–605.
[52] Alday LF, Fluder M, Sparks J. The large N limit of M2-branes on Lens spaces. J High Energy Phys 2012;2012:57. https://doi.org/10.1007/JHEP10(2012)057.
[53] Bilger RW, Stårner SH, Kee RJ. On reduced mechanisms for methaneair combustion in nonpremixed flames. Combust Flame 1990;80:135–49. https://doi.org/10.1016/0010-2180(90)90122-8.
[54] Kazakov A, Frenklach M. Reduced reaction set based on GRI-Mech 1.2: DRM19. http://combustion.berkeley.edu/drm (accessed March 26, 2023).
[55] Bergmann V, Meier W, Wolff D, Stricker W. Application of spontaneous Raman and Rayleigh scattering and 2D LIF for the characterization of a turbulent CH4/H2/N2 jet diffusion flame. Appl Phys B Lasers Opt 1998;66:489–502. https://doi.org/10.1007/s003400050424.
[56] Hafid M, Hebbir N, Lacroix M, Joly P. Simulating of non-premixed turbulent combustion using a presumed probability density function method. Heat Mass Transf 2023;59(1):81–93.
[57] Li Z, Malik MR, Cuoci A, Parente A. Edcsmoke: A new combustion solver for stiff chemistry based on OpenFOAM®. AIP Conf Proc 2017;1863:17–21. https://doi.org/10.1063/1.4992364.
[58] Cuoci A, Frassoldati A, Faravelli T, Ranzi E. OpenSMOKE++: An object-oriented framework for the numerical modeling of reactive systems with detailed kinetic mechanisms. Comput Phys Commun 2015;192:237–64. https://doi.org/10.1016/j.cpc.2015.02.014.
[59] Doan NAK, Swaminathan N. Autoignition and flame propagation in non-premixed MILD combustion. Combust Flame 2019;201:234–43. https://doi.org/10.1016/j.combustflame.2018.12.025.
[60] Vilfayeau S, Ren N, Wang Y, Trouvé A. Numerical simulation of under-ventilated liquid-fueled compartment fires with flame extinction and thermally-driven fuel evaporation. Proc Combust Inst 2015;35:2563–71. https://doi.org/10.1016/j.proci.2014.05.072.
[61] Byggstøyl S, Magnussen BF. A model for flame extinction in turbulent flow. Proc. 4th Symp. Turbul. Shear Flows., Karlsruhe, Germany: 1983, p. 10.23-10.38.